EFFECTS OF LAMINAR BURNING VELOCITY AND SPARK TIMING ON PERFORMANCE AND NO_X EMISSIONS OF A PURE AMMONIA MOTORCYCLE ENGINE

ẢNH HƯỞNG CỦA TỐC ĐỘ CHÁY TẦNG VÀ GÓC ĐÁNH LỬA SỚM ĐẾN HIỆU SUẤT VÀ PHÁT THẢI NOx CỦA ĐỘNG CƠ XE MÁY SỬ DỤNG AMONIAC NGUYÊN CHẤT

Bui Van Hung[1], Le Khac Binh[2]*

[1]The University of Danang - University of Technology and Education, Vietnam
[2]Vinh University of Technology Education, Nghean, Vietnam

*Corresponding author: khacbinhktv@gmail.com

(Received: March 25, 2026; Revised: April 21, 2026; Accepted: April 29, 2026)

DOI: 10.31130/ud-jst.2026.24(5A).063E

Abstract - This study presents a three-dimensional CFD investigation of pure ammonia combustion in a high-speed motorcycle engine at 7500 rpm using ANSYS Fluent with the Zimont Turbulent Flame Closure model. A power-law laminar burning velocity correlation, accounting for in-cylinder temperature, pressure, and mixture composition, was implemented via a User-Defined Function to improve accuracy over constant-value approaches. The effects of spark advance angle (35°-50°CA BTDC) and reference laminar burning velocity (S_{L0} = 0.04-0.10 m/s) on in-cylinder pressure, peak temperature, brake power, and NO_x emissions were examined. Optimal combustion occurs at 45° CA BTDC (1.5-2 times higher than gasoline engines), achieving 4.08 kW and 311 ppm NO_x. Ammonia power remains 33-44% lower than gasoline due to lower energy density. Sensitivity analysis shows S_{L0} causes 26.6% variation in power and over 300% in NO_x. The value S_{L0}=0.07 m/s is confirmed as most consistent with recent experimental data in the literature.

Key words - Ammonia combustion; Laminar burning velocity; Spark ignition engine; Motorcycle engine; NO_x emissions.

Tóm tắt - Nghiên cứu này trình bày mô phỏng 3D CFD quá trình cháy amoniac nguyên chất trên động cơ xe máy tốc độ cao (7500 vòng/phút) bằng ANSYS Fluent và mô hình Zimont. Để tăng độ chính xác so với việc giả định giá trị hằng số, nghiên cứu đã ứng dụng hàm UDF về tốc độ cháy tầng theo định luật lũy thừa, xét đến các yếu tố áp suất, nhiệt độ xi-lanh và nồng độ hỗn hợp. Nghiên cứu tập trung phân tích ảnh hưởng của góc đánh lửa sớm (35°-50° BTDC) và tốc độ cháy tầng tham chiếu (S_{L0} = 0.04-0.10 m/s) đến áp suất, nhiệt độ cực đại, công suất phanh và phát thải NO_x. Kết quả cho thấy quá trình cháy tối ưu tại 45° BTDC (gấp 1,5-2 lần động cơ xăng), tương ứng công suất 4,08 kW và 311 ppm NO_x. Do mật độ năng lượng thấp, công suất khi dùng amoniac giảm 33-44% so với xăng. Phân tích độ nhạy chứng minh S_{L0} gây biến thiên 26,6% về công suất và trên 300% về NO_x. Giá trị S_{L0} = 0,07 m/s nhận được phù hợp nhất với dữ liệu thực nghiệm mới nhất.

Từ khóa - Quá trình cháy amoniac; Tốc độ cháy tầng; Động cơ đốt cháy cưỡng bức; Động cơ xe máy; Phát thải NO_x.

1. Introduction

Ammonia (NH_3) is widely recognized as a viable carbon-free fuel solution with immense application potential for internal combustion engines (ICEs), the maritime industry, and power generation [1-3]. The core advantage of ammonia lies in its molecular structure, which is entirely devoid of carbon atoms. Theoretically, the complete combustion of ammonia yields only nitrogen gas and water vapor. This positions ammonia as a potential carbon-neutral fuel, playing a pivotal role in fulfilling international climate commitments, such as the Paris Agreement and the Net Zero emissions target by 2050 [4-5]. Beyond its utility as a direct fuel, ammonia is often referred to as "Hydrogen Energy 2.0" or an efficient energy vector, providing a solution to the technical barriers currently facing the hydrogen economy [6-7].

With a gravimetric hydrogen content of up to 17.8%, ammonia possesses a hydrogen density approximately 50% higher than that of compressed or liquefied hydrogen [8-9]. Specifically, the volumetric energy density of liquid ammonia (approximately 13.72 MJ/m^3 or 7.1 MJ/L) is roughly 1.7 times that of liquid hydrogen [10-12]. More importantly, ammonia can be easily liquefied at relatively low pressures (around 10 bar) at ambient temperature or at -33°C under atmospheric pressure [13]. These physical characteristics render the storage and transportation of ammonia significantly safer, simpler, and more economical than those of hydrogen. Studies indicate that the cost of storing hydrogen in the form of ammonia is only about one-third of that for pure hydrogen storage, and the total transportation costs can be 10.6 to 30.2 times cheaper [14-15]. Consequently, ammonia is regarded as the most efficient medium for hydrogen storage and distribution today; it can be utilized directly or decomposed (cracked) back into hydrogen at the point of consumption through catalytic processes [16-18].

Despite the elimination of CO_2, ammonia presents alternative toxic emission challenges. The combustion process generates substantial Nitrogen Oxides (NO_x) originating from the nitrogen atoms within the fuel itself (Fuel NO_x), resulting in exhaust NO_x concentrations potentially 1.5 to 3.5 times higher than those of gasoline engines [19-20]. Furthermore, due to its low combustibility, ammonia slip-the discharge of unburned fuel into the exhaust-poses a significant risk. Ammonia is hazardous to both human health and the environment, even at low concentrations, necessitating sophisticated after-treatment systems [21-22].

The transition from traditional hydrocarbon fuels (gasoline, diesel) to ammonia represents more than a mere fuel substitution; it is a fundamental shift in power generation mechanisms. The most pronounced discrepancy lies in energy density. The lower heating value (LHV) of ammonia (18.6 MJ/kg) is less than half that of gasoline (44.5 MJ/kg) or diesel (42.5 MJ/kg). This leads to an inherent disadvantage: to generate equivalent power output, an ammonia engine exhibits a brake-specific fuel consumption (BSFC) 2 to 2.5 times higher than that of conventional engines [20]. Consequently, on-board fuel storage systems require significantly larger volumes to achieve a comparable driving range. While gasoline and diesel engines benefit from high flame speeds and superior auto-ignition quality, enabling high rotational speeds and rapid response, ammonia suffers from an extremely low laminar burning velocity and poor ignitability. As a result, baseline ammonia engines typically underperform in terms of peak power and low-end torque, while facing major hurdles during cold starts or idling [22]. However, ammonia excels in its octane number (RON > 130), which is substantially higher than that of gasoline (RON 95). This advantage allows ammonia engines to operate at higher compression ratios (potentially reaching 15-16:1, compared to 10-12:1 for gasoline) without encountering knocking, thereby partially offsetting the loss in thermal efficiency [8, 23].

The primary technical barrier of ammonia is its extremely low laminar burning velocity, which is only approximately 6-8 cm/s compared to approx. 58 cm/s for gasoline [20]. This sluggish burning velocity results in a prolonged combustion duration, thereby reducing the heat release rate and peak pressure, which hinders the engine from achieving optimal power output and leads to efficiency degradation at low loads [22]. Furthermore, the high auto-ignition temperature (approx. 650°C) and high ignition energy requirements pose severe challenges for cold starting and maintaining combustion stability, often resulting in misfire events. The narrow flammability limits also restrict the stable operating range of the engine compared to conventional fuels [23].

Despite the growing body of research on ammonia as a carbon-free fuel, a fundamental gap remains in accurately capturing the role of laminar burning velocity under realistic engine conditions. Existing studies often rely on simplified assumptions, such as constant laminar burning velocity, or are limited to low-speed engine configurations. As a result, they fail to adequately represent high-speed spark-ignition engines, where strong turbulence–chemistry interactions critically govern flame development.

In particular, the inherently low laminar burning velocity of ammonia introduces significant challenges, including delayed combustion phasing, extended burn duration, and degraded thermal efficiency. These limitations become more severe at high engine speeds, where the available time for combustion is substantially reduced. Moreover, the considerable variability of reported laminar burning velocity values in the literature further increases the uncertainty in predicting engine performance and emissions.

To address these limitations, this study provides a systematic investigation of the effects of laminar burning velocity on combustion behavior in a high-speed ammonia-fueled motorcycle engine. By incorporating a temperature- and pressure-dependent burning velocity model within a CFD framework, the work aims to quantify its impact on flame propagation, engine performance, and NO_x formation, thereby offering new insights into the reliable modeling and optimization of ammonia combustion in practical engine applications.

2. Material and method

2.1. Material

The study was conducted on a Honda motorcycle engine with a bore of 50 mm, a stroke of 55 mm, and a compression ratio of 9:1. When operating on gasoline, the engine delivers a rated power of 6.4 kW at a speed of 7500 rpm. Upon converting to ammonia fuel, the fundamental engine specifications remained unchanged.

2.2. Research Methodology

The study was conducted using numerical simulations via ANSYS FLUENT software. The computational domain encompasses the engine cylinder and combustion chamber. The fuel-air mixture introduced into the cylinder at the beginning of the compression stroke is assumed to be homogeneous. The equivalence ratio of the mixture is determined by the fuel-dependent mixture fraction (f). In-cylinder gas flow turbulence was simulated using the k-ε turbulence model. The combustion process was modeled utilizing the partially premixed combustion (PPC) model. Given that the combustion temperature exceeds 1600 K, NO_x formation was calculated based on the Zeldovich thermal mechanism. The remaining species in the combustion products were determined through reaction equilibrium kinetics.

3. Results and Discussion

3.1. Comparison of Laminar Burning Velocities between Ammonia and Gasoline

The laminar burning velocity is the most fundamental parameter characterizing the chemical kinetics of the combustion process, reflecting the self-propagation capability of the flame front within a homogeneous fuel-air mixture under quiescent (laminar) conditions. In internal combustion engine simulations, the laminar burning velocity is typically calculated using the Metghalchi and Keck correlation [24]:

$$S_L = S_{L0}\left(\frac{T}{T_0}\right)^{\alpha}\left(\frac{P}{P_0}\right)^{\beta}$$

Where $T_0 = 298$ K and $P_0 = 0.1$ Mpa are the reference temperature and pressure, respectively; S_{L0} is the laminar burning velocity at standard conditions, which is a function of the equivalence ratio ϕ; α and β represent the temperature and pressure exponents, respectively.

For gasoline, the empirical parameters were determined as follows. The standard burning velocity S_{L0} is expressed in a quadratic form:

$$S_{L0} = B_m + B_\phi(\phi - \phi_m)^2$$

with $B_m \approx 0.28 \div 0.35$ m/s at $\phi_m \approx 1.1$. The temperature and pressure exponents for gasoline are, respectively:

$$\alpha = 2.18 - 0.8(\phi - 1)$$

$$\beta = -0.16 + 0.22(\phi - 1)$$

For ammonia (NH_3), the combustion characteristics differ significantly from those of gasoline. The peak standard burning velocity of NH_3 reaches only approximately 0.07 m/s, which is about five times lower than that of gasoline [25], and is described in an exponential form:

$$S_{L0} = 0.07 \cdot \exp\left[-16 \cdot (\phi - 1.17)^2\right] \text{(m/s)}$$

The temperature exponent of NH_3 is significantly higher than that of gasoline, typically ranging from $\alpha = 2.1 \div 2.5$, reflecting the high thermal sensitivity of the ammonia burning velocity to the mixture temperature:

$$\alpha = 2.4 - 0.5(\phi - 1)$$

The pressure exponent of NH_3 exhibits a greater negative magnitude compared to that of gasoline ($\beta \approx -0.43 \div -0.30$), indicating that an increase in pressure exerts a more pronounced inhibitory effect on the laminar burning velocity:

$$\beta \approx -0.35 \text{ (the mean value at } \phi = 1.0\text{)}$$

The discrepancies in these parameters originate from the chemical nature of NH_3: the ammonia molecule possesses high N-H bond energy (391 kJ/mol), low volumetric heating value (≈ 11.2 MJ/m^3 compare with ≈ 33.5 MJ/m^3 of gasoline), and a complex combustion reaction mechanism involving NH, NH_3, and N_2H [26]. These characteristics result in a slow heat release rate and a less stable laminar flame compared to hydrocarbon fuels.

Under the actual conditions of an internal combustion engine, the combustion process occurs within a highly turbulent environment, which significantly enhances the flame propagation speed compared to laminar conditions. According to the Damköhler model, the relationship between turbulent burning velocity and laminar burning velocity is expressed in a simplified form:

$$\frac{S_T}{S_L} = 1 + C \cdot \left(\frac{u'}{S_L}\right)^n$$

where, u' is the turbulence intensity (RMS of the turbulent velocity), C is a model constant, and n typically ranges from $0.5 \div 1.0$. This formula indicates that the ratio S_T/S_L depends directly on the ratio u'/S_L: when S_L of NH_3 is significantly lower than u', this ratio becomes very large. However, this simultaneously increases the risk of flame stretch-where the flame is excessively stretched, leading to local quenching, particularly in the cylinder boundary regions where velocity gradients are high.

In actual engine operation, the turbulent burning velocity S_T is the decisive parameter for the flame front propagation speed within the combustion chamber. Consequently, it directly influences the burn duration, the profile of the cylinder pressure curve, and the thermal efficiency. It is crucial to note that the mixture burn duration is not simply proportional to S_L, but rather depends on the complex interaction between S_L, the turbulence intensity u', and the flame structure within the combustion chamber.

Figure 1 illustrates the evolution of in-cylinder pressure, temperature, and turbulent kinetic energy$k$, along with RMS u' versus crank angle for the engine operating on gasoline at $n = 7500$ rpm, $\phi = 1$, and an ignition timing of $\varphi_s = 35$°CA. The results indicate that the mixture temperature reaches its peak after the peak pressure occurs, reflecting the characteristic of an incomplete isochoric combustion process. Notably, the turbulent kinetic energy k and RMS u' reach their maximum values at approximately 320°CA- significantly lagging behind the peak pressure position - as this corresponds to the final stage of the intake process, where the induced charge causes intense turbulence within the combustion chamber. From the turbulent kinetic energy k, the turbulence intensity RMS is calculated as follows:

$$u' = \sqrt{\frac{2k}{3}}$$

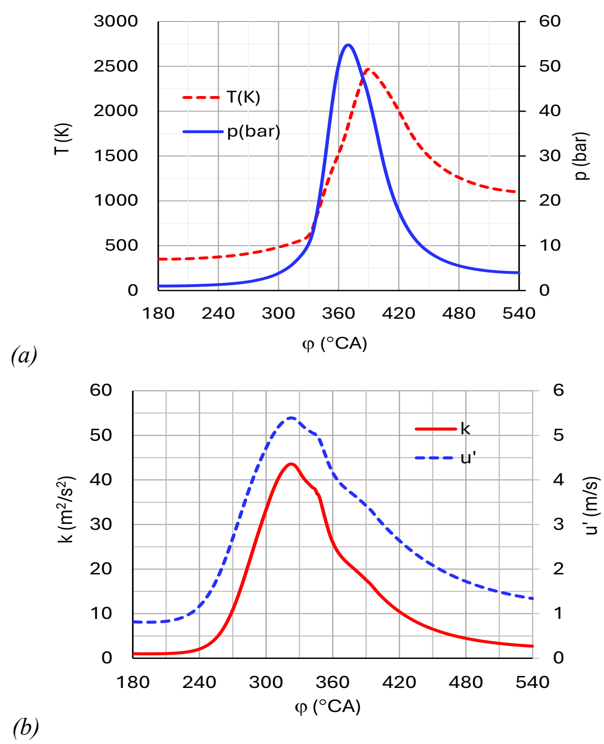

Figure 1. *Variations in in-cylinder pressure and temperature (a) and variations in turbulent kinetic energy k and RMS u' (b) versus crank angle (engine operating on gasoline, n=7500 rpm, ϕ=1, φ_s=35°CA)*

Figure 2 illustrates the evolution of laminar burning velocity S_L and turbulent burning velocity S_T versus crank angle for the engine operating on gasoline at $n = 7500$ rpm, $\phi = 1$, and $\varphi_s = 35$°CA. In this calculation, the gasoline parameters used are: $S_{L0} = 0.30$ m/s, $\alpha = 2.1$, and $\beta = -0.16$. The results show that S_L reaches a peak value of 18 m/s and S_T reaches a peak of 25.5 m/s at the 290°CA position - the moment when the in-cylinder temperature reaches its maximum. This is entirely consistent with theory: S_L increases with temperature but decreases with pressure, and at 290°CA, the temperature effect becomes dominant. Turbulent motion has enhanced the burning velocity of the fuel-air mixture by 7.5 m/s compared to laminar conditions, equivalent to a peak turbulent burning velocity 1.4 times higher than the peak laminar burning velocity.

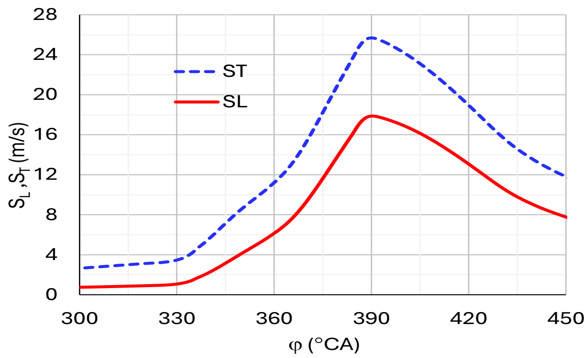

Figure 2. *Variations in laminar burning velocity (S_L) and turbulent burning velocity (S_T) versus crank angle (engine operating on gasoline, n=7500 rpm, ϕ=1, φ_s =35°CA)*

Figure 3 presents the contours of temperature (*T*), turbulence intensity (u'), and turbulent burning velocity (S_T) at crank angles of 360°CA and 380°CA for the ammonia-fueled engine at $n = 7500$ rpm, $\phi = 1$, and $\varphi_s = 50$°CA. Since the ammonia-air mixture has a much lower burning velocity than gasoline, the ignition timing of the engine must be advanced to 60°CA compared to 35°CA of gasoline. The results show that although the flame front expands during the combustion process, the turbulence intensity and turbulent burning velocity remain concentrated in the center of the combustion chamber. This is explained by the low burning velocity of ammonia, which prolongs the combustion duration, leading to a gradual decrease in the burning rate toward the end of the process. Consequently, a portion of the mixture near the cylinder walls remains unburned-this is the primary cause of heat loss and reduced engine efficiency when using pure ammonia.

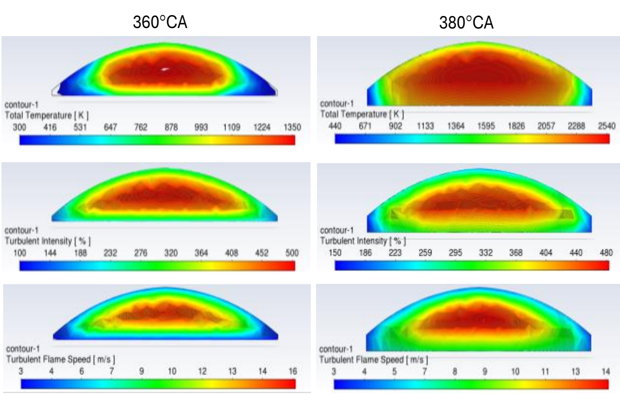

Figure 3. *Contours of temperature T, turbulence intensity u', and turbulent burning velocity S_T at crank angles of 360°CA (a) and 380°CA (b) (Ammonia engine, n=7500 rpm, ϕ=1, φ_s =50°CA)*

Figure 4 presents the simulation results for the evolution of in-cylinder pressure, temperature, and turbulent parameters (k, u' and S_L, S_T) for the engine operating on ammonia at $n = 7500$ rpm, with the following parameters: $S_{L0} = 0.07$ m/s, $\alpha = 2.4$, $\beta = -0.45$. Compared to the gasoline case, the peak in-cylinder pressure and temperature decrease significantly when running on ammonia. This can be attributed to three primary reasons: (i) the lower heating value of the NH_3-air mixture compared to the gasoline-air mixture; (ii) the reduction in volumetric efficiency as ammonia occupies a larger volume in the intake charge; and (iii) the prolonged combustion process leading to incomplete combustion. The turbulent kinetic energy and RMS reach their peaks at the same crank angle as the gasoline engine, but the values are approximately 1 m/s lower due to the lower rate of pressure rise in the combustion chamber, which reduces the turbulent effects hindering flame front propagation. Notably, the peak laminar burning velocity S_L reaches 3.5 m/s, while the peak turbulent burning velocity S_T reaches 7.1 m/s. Consequently, the S_T/S_L ratio for ammonia reaches 2.0, significantly higher than that of gasoline (1.4 times), reflecting the more critical role of turbulence in enhancing the burning rate when using low S_L fuels.

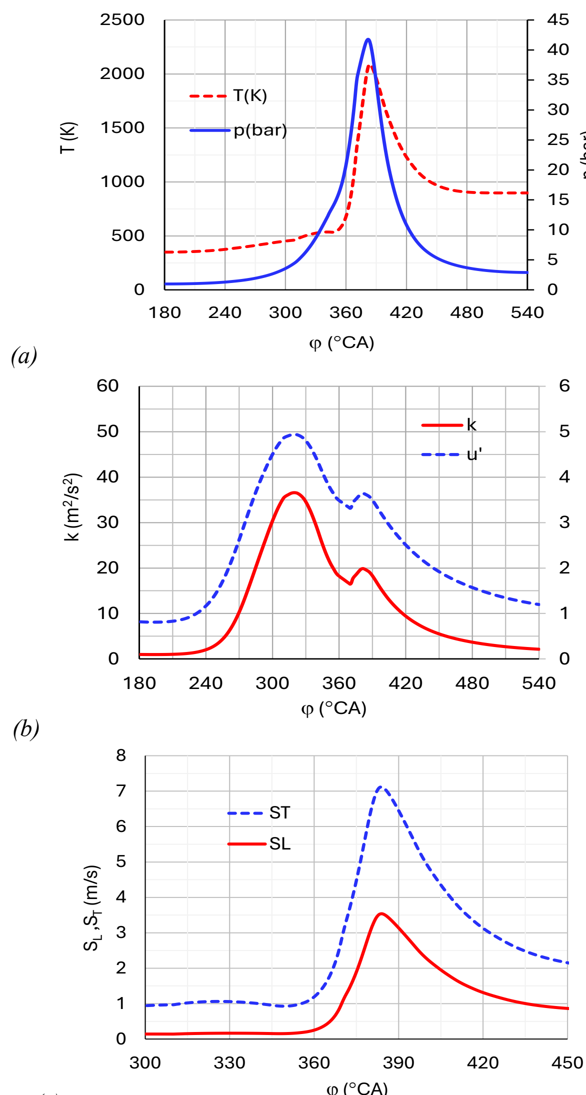

Figure 4. *Variations in in-cylinder pressure and temperature (a), k and u' (b) and S_L, S_T (c) versus crank angle for the ammonia-fueled engine at n=7500 rpm, ϕ=1, φ_s =50°CA*

3.2. Effects of ignition timing on ammonia engine performance

As the laminar burning velocity of ammonia is approximately five times lower than that of gasoline, the combustion process in an NH_3-fueled engine occurs significantly slower. This necessitates advancing the ignition timing to ensure that combustion is completed near TDC, thereby optimizing the indicated work. This remains one of the most critical technical challenges when retrofitting gasoline engines to operate on pure ammonia. In this study, the effects of advanced ignition timing φ_s were investigated at four values: 35°CA, 40°CA, 45°CA and 50°CA BTDC, at an engine speed of $n = 7500$ rpm and an equivalence ratio of $\phi = 1$.

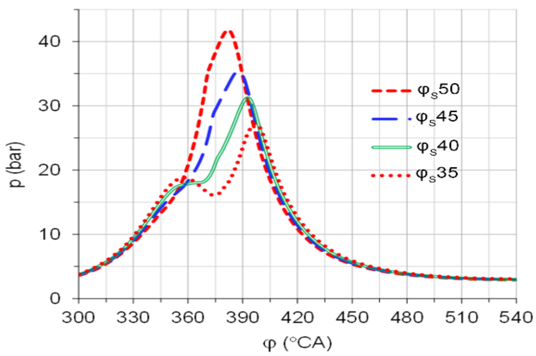

(a)

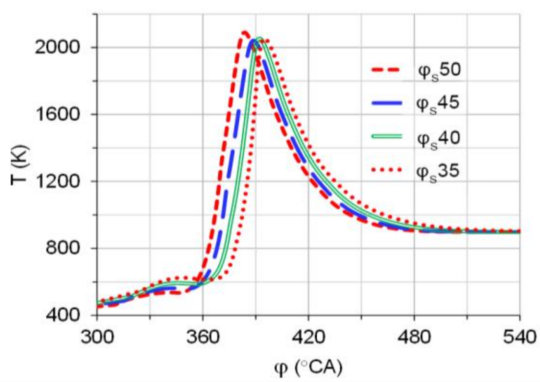

(b)

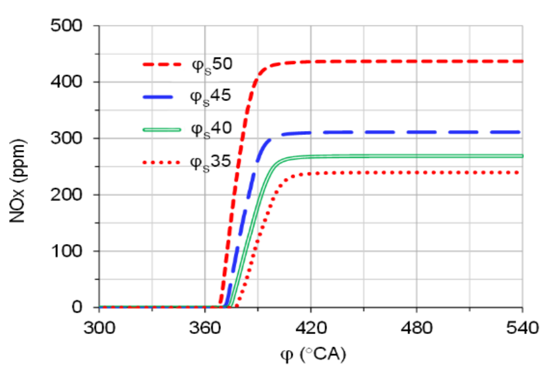

(c)

Figure 5. *Effects of ignition timing on the variations in in-cylinder pressure (a), temperature (b), and NO_x concentration (c) versus crank angle for the ammonia-fueled engine at $n = 7500$ rpm and $\phi=1$*

Figure 5a illustrates the evolution of in-cylinder pressure versus crank angle for different ignition timings. The results show that the peak pressure P_{max} increases significantly with an advanced ignition timing. Specifically, when φ_s increase from 35°CA to 50°CA, then P_{max} increases from 27.24 bar to 41.79 bar - a 53.4% enhancement. This is entirely consistent with theory: with an advanced ignition timing, the combustion process occurs while the piston is still ascending, thereby increasing the combined compression pressure and shifting the peak pressure closer to TDC, where the combustion chamber volume is at its minimum. Similar results have been reported in studies on spark-ignition engines fueled by ammonia, where the optimum ignition timing typically ranges from 40° ÷ 60°CA BTDC, depending on engine speed and load.

The peak combustion temperature T_{max} exhibits a positive correlation with the spark advance angle, escalating from 2043 K at $\varphi_s = 45°$ CA to 2090 K at $\varphi_s = 50°$ CA, as illustrated in Figure 5b and Table 1. However, the increment in T_{max} is non-monotonic: specifically, as SA shifts from 35° to 40° CA BTDC, T_{max} undergoes a marginal decline from 2056 K to 2054 K, followed by a robust surge to 2090 K at $\varphi_s = 50°$ CA BTDC. This behavior stems from a trade-off between two competing mechanisms: (i) advanced ignition elevates temperatures by initiating combustion in closer proximity to TDC; (ii) conversely, excessive advancement triggers premature heat release while the piston is still ascending, thereby increasing compression work (negative work) and inducing an irregular temperature profile. The exhaust gas temperature $T_{Exhaust}$ remains relatively stable at 898 K for $\varphi_s = 40° \div 50°$CA, but rises slightly to 904 K at $\varphi_s = 35°$CA. This suggests that retarded ignition promotes late-phase combustion extending into the expansion stroke, resulting in higher thermal energy discharge.

Table 1 summarizes the engine performance metrics across the investigated ignition range. The indicated work per cycle increases progressively from 68.79 J/cycle ($\varphi_s = 35°$CA) to 81.2 J/cycle ($\varphi_s = 50°$CA), corresponding to a brake power P_e enhancement from 3.61 kW to 4.26 kW. Consequently, within the scope of this study, a spark advance of $\varphi_s = 50°$CA yields the optimal power output.

Table 1. *Summary of ammonia-fueled engine performance characteristics as a function of spark advance angle ($n = 7500$ rpm, $\phi = 1$)*

Symbol	$\varphi_s = 35°$	$\varphi_s = 40°$	$\varphi_s = 45°$	$\varphi_s = 50°$
P_{max}(bar)	27.24	31.23	35.27	41.79
T_{max}(K)	2056	2054	2043	2090
$T_{Exhaust}$(K)	904	898	898	898
W_i(J/cyc.)	68.79	73.62	77.8	81.2
P_e(kW)	3.61	3.87	4.08	4.26
NO_x (ppm)	240	269	311	437
ΔP_e comparison with gasoline (%)	43.59	39.53	36.25	33.44

Compared to the gasoline engine under identical operating conditions ($P_e^{gasoline} = 6.4$ kW at $n = 7500$ rpm), the power output of the ammonia-fueled engine significantly decreases across all investigated spark advance angles. The power reduction ΔP_e ranges from 33.44% ($\varphi_s = 50°$CA) to 43.59% ($\varphi_s = 35°$CA). This degradation is primarily attributed to the lower volumetric heating value of the ammonia-air mixture ($\approx 11.2\,\mathrm{MJ/m^3}$) relative to the gasoline-air mixture ($\approx 33.5\,\mathrm{MJ/m^3}$), compounded by a reduced volumetric efficiency as ammonia occupies a substantial fraction of the intake charge. These findings align with recent publications on ethanol-ammonia motorcycle engines, which conclude that power loss with neat ammonia is inevitable without turbocharging or mixture enrichment measures.

Notably, the rate of power enhancement with respect to the spark advance angle exhibits a diminishing trend: increasing φ_s from 35° to 40° yields a 0.26 kW gain, whereas subsequent increments from 40° to 45° and 45° to 50° result in gains of only 0.21 kW and 0.18 kW, respectively. This trend suggests that the power curve $P_e(\varphi_s)$ is approaching its peak-the maximum brake torque (MBT) timing-at an ignition angle beyond 50°CA. However, further advancement of the φ_s is constrained by the risk of engine knock and, more critically, a sharp escalation in NO_x emissions, as analyzed in the following section.

Figure 5c and Table 1 illustrate a profound escalation in exhaust NO_x concentrations as the spark advance angle increases, rising from 240 ppm ($\varphi_s = 35°\mathrm{CA}$) to 437 ppm ($\varphi_s = 50°\mathrm{CA}$) - representing an 82% increase over a 15°CA increment. This highlights a fundamental trade-off in ammonia engine optimization: while a larger spark advance enhances power output, it simultaneously triggers a sharp surge in NO_x emissions.

The NO_x formation mechanism in ammonia-fueled engines differs significantly from that of conventional hydrocarbon engines. In addition to the thermal NO_x mechanism (Zeldovich mechanism), which is highly temperature-dependent, NH_3 combustion involves the fuel NO_x mechanism. In this pathway, NO_x originates directly from the nitrogen atoms within the ammonia molecule through the following reaction pathways:

$$\mathrm{NH_3 + O \rightarrow NH_2 + OH}$$
$$\mathrm{NH_2 + O \rightarrow NO + H_2}$$
$$\mathrm{NH + O \rightarrow NO + H}$$

The fuel NO_x mechanism renders NO_x emissions from ammonia-fueled engines exceptionally sensitive to combustion temperature and the residence time of the mixture at elevated temperatures. As the spark timing is advanced from 45°CA to 50°CA BTDC, T_{max} increases from 2043 K to 2090 K (an increment of 47 K), yet NO_x emissions surge from 311 ppm to 437 ppm (a 40.5% increase). This reflects the exponential dependence of the NO_x formation rate on temperature according to the Arrhenius equation, particularly in temperature regions exceeding 2000 K.

These results necessitate a multi-objective optimization approach: identifying the optimal spark timing that balances power output and emissions. Data analysis indicates that at $\varphi_s = 45°\mathrm{CA}$, the engine achieves a relatively reasonable compromise: the power output $P_e = 4.08\,\mathrm{kW}$ (a 36.25% reduction compared to gasoline) is maintained with NO_x at 311 ppm - significantly lower than at $\varphi_s = 50°\mathrm{CA}$ (437 ppm) while the power decrease is negligible at only 0.18 kW. This observation is consistent with existing studies on spark timing optimization for ammonia engines, where the optimal operating point is typically determined based on the BSFC-NO_x trade-off index.

3.3. Influence of Laminar Burning Velocity (S_{L0})

The laminar burning velocity at reference conditions (298 K and 1 bar) is a critical parameter for calculating the laminar burning velocity under the wide-ranging pressures and temperatures encountered within the engine combustion chamber. This parameter is highly sensitive, significantly affecting both engine performance and pollutant emission levels. As S_{L0} varies, the spark timing must be adjusted accordingly to ensure that engine performance parameters reach their optimal values.

As analyzed in the previous sections, the laminar burning velocity S_L plays a fundamental role throughout the entire engine combustion process. It not only directly determines the turbulent burning velocity S_T through the ratio S_T/S_L, but also influences the optimal spark timing. Consequently, it impacts the entire chain of parameters: from the pressure curve profile to the indicated work, brake power, and ultimately, NO_x emissions. Among the parameters of S_L, the reference value S_{L0} at standard conditions ($T_0 = 298\,\mathrm{K}$, $P_0 = 0.1\,\mathrm{MPa}$) is the most sensitive parameter, as it serves as the scaling factor for the entire burning velocity field within the combustion chamber according to the following formula:

$$S_L = S_{L0}\left(\frac{T}{T_0}\right)^{\alpha}\left(\frac{P}{P_0}\right)^{\beta}$$

Of particular significance regarding ammonia is that the S_{L0} values of NH_3 currently exhibit considerable dispersion among various experimental literature sources. Direct measurement studies indicate that the S_{L0} of NH_3 at reference conditions fluctuates within the range of 0.05 ÷ 0.09 m/s, depending on the measurement technique, experimental conditions, and the kinetic mechanism employed [27]. This dispersion is substantially larger than those observed for gasoline or methane, originating from the unique chemical properties of NH_3: slow reaction rates, thin flame thickness, and high susceptibility to the stretch effect [28]. Consequently, evaluating the sensitivity of engine simulation results to S_{L0} is an indispensable validation step before concluding the performance of ammonia-fueled engines.

In this section, four S_{L0} values are investigated: 0.04, 0.06, 0.07, and 0.10 m/s, covering the entire range of values reported in the literature. For each S_{L0} value, the spark timing is adjusted accordingly to achieve optimal performance, consistent with the methodology presented. All calculations are performed at $= 7500$ rpm, $\phi = 1$, $\varphi_s = 50°\mathrm{CA}$.

Figure 6a presents the cylinder pressure curves p-V versus combustion chamber volume for the four S_{L0} values. The results indicate a significant increase in peak pressure P_{max}) as S_{L0} increases. Specifically, according to Table 2, when S_{L0} is raised from 0.04 m/s to 0.10 m/s, P_{max} surges from 38.42 bar to 47.25 bar - representing a 23.0% increment. This substantial increase reflects a clear physical mechanism: a higher S_{L0} leads to a higher S_L across all T, P conditions, which in turn results in a higher S_T. This accelerates flame propagation, allowing the combustion process to be completed earlier and more concentrated near the TDC, ultimately leading to higher peak pressure and a larger area within the indicator diagram p-V.

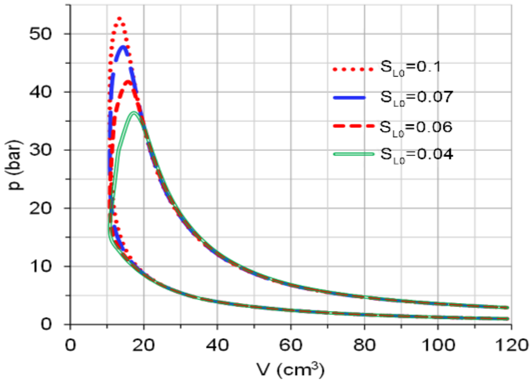

(a)

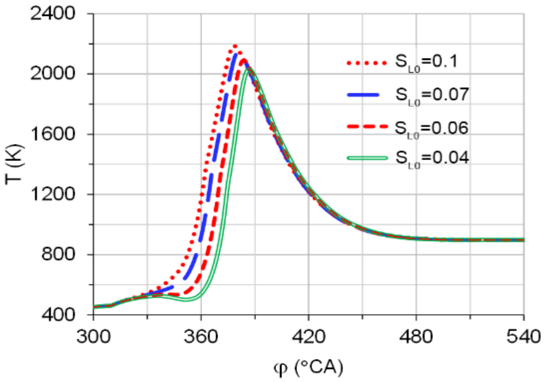

(b)

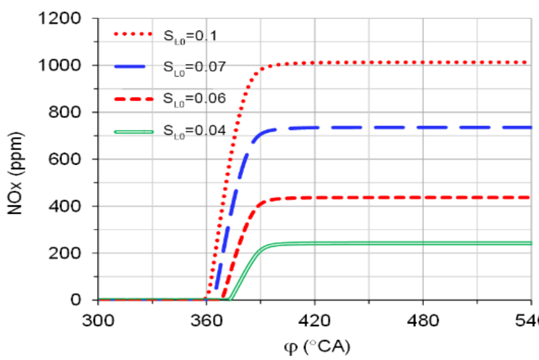

(c)

Figure 6. *Influence of the ammonia laminar burning velocity at reference conditions, S_{L0} (298 K, 1 bar), on the variations of cylinder pressure (a), temperature (b), and NO_x concentration versus combustion chamber volume, operating at an engine speed of 7500 rpm, ϕ=1. φ_s=50°CA*

Table 2. *Summary of ammonia engine performance parameters according to the S_{L0} values ($n = 7500$ rpm, $\phi = 1$, $\varphi_s = 60°CA$)*

Symbol	S_{L0} = 0.04	S_{L0} = 0.06	S_{L0} = 0.07	S_{L0} = 0.10
P_{max}(bar)	38.42	41.72	41.79	47.25
T_{max}(K)	2030	2030	2090	2140
$T_{exhaust}$(K)	898	898	898	898
W_i(J/cyc.)	70.86	76.96	81.2	84.2
P_e(kW)	3.49	4.04	4.25	4.42
NO_x (ppm)	-	240	437	730
ΔP_e comparison with gasoline (%)	45.47	36.88	33.59	30.94

Figure 6b shows that the peak temperature (T_{max}) also increases with S_{L0}, rising from 2030 K (at $S_{L0} = 0.04$ m/s) to 2140 K (at $S_{L0} = 0.10$ m/s). Notably, the exhaust gas temperature T_{thai} remains stable at 898 K across all cases, indicating that the fraction of heat energy dissipated via exhaust emissions does not change significantly; the primary difference lies in the amount of heat energy converted into mechanical work. This observation is consistent with the findings of Lhuillier et al. [29], who stated that in ammonia engines, the thermal conversion efficiency depends more heavily on the laminar burning velocity than on the fuel's heating value.

The indicated cycle work W_i and brake power P_e increase monotonically with S_{L0}, rising from 3.49 kW (at $S_{L0} = 0.04$ m/s) to 4.42 kW (at $S_{L0} = 0.10$ m/s). However, it is noteworthy that the rate of power increase relative to S_{L0} is non-linear: when S_{L0} increases from 0.04 to 0.06 m/s (a 50% increase), the power output P_e rises by 0.55 kW (15.8% increase), whereas when S_{L0} increases from 0.06 to 0.10 m/s (a 67% increase), P_e only gains an additional 0.38 kW (9.4% increase). This trend reflects a gradual saturation of the influence of S_{L0} on engine performance at higher values: once S_T is sufficiently large, the combustion process is already completed near the TDC, and further increases in S_{L0} no longer significantly improve the combustion phasing [21].

When compared to the gasoline engine ($P_e^{gasoline} =$ 6.4 kW), the power reduction ΔP_e remains substantial even at $S_{L0} = 0.10$ m/s: 30.94%. This confirms that even in the most optimistic scenario regarding ammonia burning velocity, the power drop relative to gasoline is an inherent challenge stemming from the low volumetric heating value of NH_3, which cannot be overcome solely by optimizing spark timing. This is consistent with the conclusion by D'Antuono [21] that restoring ammonia engine power to levels comparable with gasoline requires a simultaneous combination of multiple solutions: increasing intake pressure, hydrogen (H_2) enrichment, or employing multi-spark ignition strategies.

Figure 6c and Table 2 show that NO_x emissions surge aggressively with S_{L0}, rising from 240 ppm (at $S_{L0} =$ 0.06 m/s) to 730 ppm (at $S_{L0} = 0.10$ m/s)-a more than threefold increase while S_{L0} did not even double. This result holds significant scientific weight, reflecting the non-linear interaction between S_{L0}, combustion temperature, and the specific NO_x formation mechanisms of ammonia.

The explanatory mechanism can be analyzed from two perspectives. First, a higher S_{L0} leads to a higher T_{max} (from 2030 K to 2140 K), which strongly activates the thermal NO_x mechanism (Zeldovich) with a formation rate that depends exponentially on temperature. Second, and more critically for ammonia, a higher S_{L0} signifies a more complete combustion process-meaning more NH_3 molecules are thoroughly oxidized, thereby increasing the contribution of the fuel NO_x mechanism through the reaction chain [28]:

$$NH_3 \overset{+O,OH}{\rightarrow} NH_2 \overset{+O}{\rightarrow} NH \overset{+O}{\rightarrow} NO$$

These results present a simultaneous tri-objective optimization problem: power output - NO_x emissions - and S_{L0} uncertainty. Data analysis shows that at $S_{L0} = 0.07$ m/s - a value validated by numerous independent experimental studies-the engine achieves a reasonable balance: $P_e = 4.25$ kW with NO_x = 437 ppm. This value is also utilized as the reference point throughout this entire study.

The sensitivity analysis results in this section hold significant practical implications for the ammonia engine simulation research community. Variations within the 0.04 ÷ 0.10 m/s range-which falls entirely within the uncertainty bounds of existing experimental data [27] lead to a 26.6% change in power and a more than threefold increase in NO_x. This implies that ammonia engine simulation results are extremely sensitive to the S_{L0} input value, and any conclusions regarding performance or emissions must be evaluated within the context of this uncertainty range. This observation is consistent with the analysis by Mashruk et al. [28], where errors $\pm 10\%$ in S_{L0} can cause up to a 14% error in turbulent burning velocity and tens of percent in NO_x prediction.

From an experimental perspective, these results emphasize the necessity for precise measurement S_{L0} of NH_3 at elevated pressure and temperature conditions-closely mimicking the actual environment within the engine combustion chamber-rather than relying solely on atmospheric measurements [27]. This remains one of the high-priority research directions in the field of ammonia engines today.

4. Conclusion

This study presents the results of a three-dimensional CFD simulation of pure ammonia combustion in a high-speed motorcycle engine (7500 rpm) using ANSYS Fluent software. The key conclusions are drawn as follows:

- Due to the inherently low laminar burning velocity of NH_3, which is approximately 5 to 7 times lower than that of gasoline-the combustion of pure ammonia in high-speed motorcycle engines requires significantly advanced spark timing, specifically within the range of $45° \div 50°$ CA BTDC. This is essential to ensure that combustion is completed near the TDC and to maximize the indicated work. This timing is 1.5 to 2 times larger than the conventional spark timing for gasoline engines operating at equivalent speeds.

- At the determined optimal spark timing of $\varphi_s = 45°$ CA BTDC, the engine achieves a brake power of $P_e = 4{,}08$ kW with NO_x emissions of 311 ppm, representing the most favorable balance between power output and pollutant emissions. Further advancing the spark timing to 50°CA results in only a marginal power increase to 4.26 kW, while NOx emissions surge to 437 ppm (a 40.5% increase). This surge is attributed to the simultaneous activation of both thermal NO_x and fuel NO_x mechanisms unique to nitrogen-based fuels.

- Across all investigated spark timings, the brake power of the pure ammonia engine remains 33-44% lower than that of the baseline gasoline engine ($P_e^{gasoline} = 6{,}4$ kW), primarily due to the low volumetric heating value of the NH_3-air mixture. This power deficit cannot be rectified solely through spark timing optimization, necessitating additional solutions such as mild boosting, hydrogen enrichment, or multi-spark ignition strategies for practical motorcycle applications.

- Sensitivity analysis over the S_{L0} range of 0.04 m/s to 0.1 m/s - covering the full spectrum of existing experimental data-demonstrates that uncertainty in this single parameter leads to a 26.6% variation in power and over a 300% variation in NO_x emissions. These results clearly indicate that the predictive accuracy of ammonia engine simulations is fundamentally limited by the dispersion of current experimental data, emphasizing the urgent need for precise measurements of NH_3 laminar burning velocity at elevated pressures and temperatures.

- The reference value of $S_{L0} = 0.07$ m/s at stoichiometric conditions (298 K, 0.1 MPa) is confirmed as the most consistent choice relative to recent experimental literature, providing simulation results that align well with reported trends for ammonia-fueled SI engines. The use of this value is recommended for future CFD studies on pure ammonia combustion.

- From a practical application perspective, utilizing pure ammonia as a direct alternative fuel for high-speed motorcycle engines is technically feasible but requires the simultaneous implementation of several measures: (i) an adaptive spark timing control system within the $45° \div 55°$ CA BTDC range, (ii) post-engine NO_x treatment via selective catalytic reduction (SCR) or exhaust gas recirculation (EGR), and (iii) power restoration strategies. Hydrogen enrichment with NH_3 represents the most promising short-term direction to concurrently improve burning velocity, reduce NO_x through De-NO_x reactions, and restore engine power to levels comparable with gasoline.

Acknowledgement: This work was supported by the Ministry of Education and Training of Vietnam through the research project "Investigation and Development of an Extended-Range Electric Motorcycle (EREM) Powered by a Hydrogen carrier fuel Engine," Code: B2026-DNA-09.

REFERENCES

[1] U. Kalim, *et al.*, *Powertrain Systems for a Sustainable Future* - Chapter: Combustion analysis of ammonia and methanol fuels and their blends in an optical spark-ignition engine, CRC Press, pp. 125-138, 2023. DOI:10.1201/9781032687568-7

[2] A. Doosti, *et al.*, "A critical review on ammonia as a fuel for internal combustion engines: Is it a viable option?", *Renewable and Sustainable Energy Reviews,* vol. 222, 115964, 2025. https://doi.org/10.1016/j.rser.2025.115964

[3] P. Dong, *et al.*, "Future zero carbon ammonia engine: Fundamental study on the effect of jet ignition system characterized by gasoline ignition chamber", *Journal of Cleaner Production,* vol. 435, 2024. https://doi.org/10.1016/j.jclepro.2023.140546

[4] K. Laveet and A. K. Sleiti, "Systematic review on ammonia as a sustainable fuel for combustion", *Renewable and Sustainable Energy Reviews,* vol. 202, 2024. https://doi.org/10.1016/j.rser.2024.114699

[5] L. Zongkuan, L. Zhou, and H. Wei, "Experimental investigation on

the performance of pure ammonia engine based on reactivity controlled turbulent jet ignition", *Fuel,* vol. 335, 2023. https://doi.org/10.1016/j.fuel.2022.127116

[6] R. Novella, *et al.* "Numerical study on the use of ammonia/hydrogen fuel blends for automotive spark-ignition engines", *Fuel,* vol. 351, 2023. https://doi.org/10.1016/j.fuel.2023.128945

[7] T. F. Guiberti, *et al*. "Mini review of ammonia for power and propulsion: advances and perspectives", *Energy & Fuels,* vol. 37, pp. 14538-14555, 2023. https://doi.org/10.1021/acs.energyfuels.3c01897

[8] C. Lhuillier, *et al.,* "Experimental study on ammonia/hydrogen/air combustion in spark ignition engine conditions", *Fuel,* vol. 269, 2020. https://doi.org/10.1016/j.fuel.2020.117448

[9] C. Zamfirescu and I. Dincer, "Ammonia as a green fuel and hydrogen source for vehicular applications", *Fuel processing technology,* vol. 90, pp. 729-737, 2009. https://doi.org/10.1016/j.fuproc.2009.02.004

[10] L. Herry, *et al.* "NH_3 as a transport fuel in internal combustion engines: a technical review", *Journal of Energy Resources Technology*, vol. 141, 2019. https://doi.org/10.1115/1.4042915

[11] D. R. MacFarlane, *et al.,* "A roadmap to the ammonia economy", *Joule,* vol. 4, pp. 1186-1205, 2020.

[12] R. Kyunghyun, G. E. Zacharakis-Jutz, and S. C. Kong, "Performance enhancement of ammonia-fueled engine by using dissociation catalyst for hydrogen generation", *International journal of hydrogen energy,* vol. 39, pp. 2390-2398, 2014. https://doi.org/10.1016/j.ijhydene.2013.11.098

[13] I. Haris and C. Crawford, "Review of ammonia production and utilization: Enabling clean energy transition and net-zero climate targets", Energy Conversion and Management, vol. 300, 2024. https://doi.org/10.1016/j.enconman.2023.117869

[14] C. Zamfirescu, and I. Dincer, "Using ammonia as a sustainable fuel", *Journal of Power Sources,* vol. 185.1, pp. 459-465, 2008. https://doi.org/10.1016/j.jpowsour.2008.02.097

[15] Y. Arda and I. Dincer, "A review on clean ammonia as a potential fuel for power generators", *Renewable and sustainable energy reviews,* vol. 103, pp. 96-108, 2019. https://doi.org/10.1016/j.rser.2018.12.023

[16] M. Shreya, *et al.,* "Low-temperature ammonia decomposition catalysts for hydrogen generation", *Applied Catalysis B: Environmental,* vol. 226, pp. 162-181, 2018. https://doi.org/10.1016/j.apcatb.2017.12.039

[17] W. Du, *et al.,* "Numerical study of the premixed ammonia-hydrogen combustion under engine - relevant conditions", *International Journal of Hydrogen Energy,* vol. 46, pp. 2667-2683, 2021. https://doi.org/10.1016/j.ijhydene.2020.10.045

[18] C. Wai Siong, *et al*. "A review on ammonia, ammonia-hydrogen and ammonia-methane fuels", *Renewable and Sustainable Energy Reviews,* vol. 147, 2021. https://doi.org/10.1016/j.rser.2021.111254

[19] M. Xiangyu, *et al.,* "Understanding of combustion characteristics and NO generation process with pure ammonia in the pre-chamber jet-induced ignition system", *Fuel*, vol. 331, 2023. https://doi.org/10.1016/j.fuel.2022.125743

[20] W. Zhihong*, et al.,* "Systematic assessment on the ammonia/gasoline combustion performance in a modern dual-fuel spark-ignition engine on different conditions", *Fuel,* vol. 392, 2025. https://doi.org/10.1016/j.fuel.2025.134806

[21] G. d'Antuono, *et al.,* "Assessment of combustion development and pollutant emissions of a spark ignition engine fueled by ammonia and ammonia-hydrogen blends", *International Journal of Hydrogen Energy,* vol 85, pp. 191-199, 2024. https://doi.org/10.1016/j.ijhydene.2024.08.210

[22] L. Shang, *et al.,* "Combustion and emission characteristics of a gasoline/ammonia fueled SI engine and chemical kinetic analysis of NO_x emissions", *Fuel,* vol. 367, 2024. https://doi.org/10.1016/j.fuel.2024.131516

[23] S. Jiuling, *et al*., "Combustion characteristics and flame development of ammonia in an optical spark-ignition engine", *Fuel,* vol. 375, 2024. https://doi.org/10.1016/j.fuel.2024.132601

[24] M. Metghalchi and J. C. Keck. "Laminar burning velocity of propane-air mixtures at high temperature and pressure", *Combustion and flame,* vol. 38, pp. 143-154, 1980. https://doi.org/10.1016/0010-2180(80)90046-2

[25] H. Akihiro, *et al.,* "Laminar burning velocity and Markstein length of ammonia/air premixed flames at various pressures", *Fuel,* vol. 159, pp. 98-106, 2015. https://doi.org/10.1016/j.fuel.2015.06.070

[26] V. M Agustin, *et al.,* "Review on ammonia as a potential fuel: from synthesis to economics", *Energy & Fuels*, vol. 35, pp. 6964-7029, 2021. https://doi.org/10.1021/acs.energyfuels.0c03685

[27] L. F. Alvarez, *et al*., "Laminar burning velocity of Ammonia/Air mixtures at high pressures", *Fuel,* vol. 363, 2024. https://doi.org/10.1016/j.fuel.2024.130986

[28] M. Syed, *et al*., "Perspectives on NO_x emissions and impacts from ammonia combustion processes", *Energy & Fuels*, vol. 38, pp. 19253-19292, 2024. https://doi.org/10.1021/acs.energyfuels.4c03381

[29] L. Charles, *et al.,* "Experimental study on ammonia/hydrogen/air combustion in spark ignition engine conditions", *Fuel*, vol. 269, 2020. https://doi.org/10.1016/j.fuel.2020.117448

[30] B. V. Hung, *et al*., "AI-assisted ecu programming for twining injectors supplying flexible syngas-biogas-hydrogen blend to engines*", The University of Danang - Journal of Science and Technology*, vol. 23, no. 12, 2025. https://doi.org/10.31130/ud-jst.2025.23(12).693E

[31] B. V. Ga, *et al.,* "Refuse derived fuel (RDF) combustion in atmospheric conditions: a simulation study", *The University of Danang - journal of science and technology,* vol. 22, No. 5A, 2024.